



## Nanoelectrode Ensembles Using Carbon Nanopipettes

Randall D. Lowe,<sup>a,c,\*</sup> Radhika C. Mani,<sup>a,d</sup> Richard P. Baldwin,<sup>b</sup> and Mahendra K. Sunkara<sup>a,\*,z</sup>

<sup>a</sup>Department of Chemical Engineering, and <sup>b</sup>Department of Chemistry, University of Louisville, Louisville, Kentucky 40292, USA

We demonstrate a simple approach for fabricating nanoelectrode ensembles (NEEs) for nanostructures exhibiting conical morphologies. The fabrication concept utilizes the tapered geometries of carbon nanopipettes (CNPs) and entails one simple, dip-coating step with an insulating polymer to engineer their spatial distribution. After dip-coating, the CNPs in the NEE are separated by several micrometers. Uncoated CNP arrays exhibit peak-shaped behavior in cyclic voltammetry, whereas polymer-coated NEEs yield steady-state, sigmoidal voltammograms over a wide range of scan rates. As-synthesized CNPs could also be employed as templates for synthesizing conical morphologies of other materials to be incorporated into NEEs.

© 2006 The Electrochemical Society. [DOI: 10.1149/1.2193071] All rights reserved.

Manuscript submitted September 27, 2005; revised manuscript received February 10, 2006. Available electronically April 7, 2006.

Nanoelectrodes, with their small critical dimensions, possess many advantages over their larger, macro-sized electrode counterparts.<sup>1,2</sup> Nanoelectrodes are desirable because they exhibit radial diffusion,<sup>1</sup> the rapid attainment of steady-state currents,<sup>3</sup> increased signal to background ratios,<sup>4</sup> higher sensitivities,<sup>4,5</sup> and decreased effects from ohmic potential drop<sup>6</sup> compared to larger electrodes. In addition, nanoelectrodes have direct applications in resolving the kinetics of rapid electron transfer reactions,<sup>7</sup> the *in vivo* detection of biologically significant compounds such as neurotransmitters on short time scales,<sup>8</sup> and even in imaging as in scanning electrochemical microscopy (SECM).<sup>1</sup> Nanoelectrode ensembles (NEEs) have the advantage of packaging thousands of individual nanoscale elements into single devices that are easily manipulated and yield higher signals while still maintaining the performance enhancements obtained from single nanoelectrodes.<sup>1</sup>

However, NEE fabrication is no trivial task. NEEs have been fabricated with a variety of methods including the use of templates and self-assembled monolayers.<sup>1,9</sup> Koehne et al. fabricated nanoelectrode arrays (NEAs) using multiwalled carbon nanotubes (CNTs),<sup>5</sup> but their technique required a series of micro/nanofabrication procedures. Here, a new NEE fabrication method is presented that avoids the complications of microfabrication, template-assisted, and self-assembled monolayer (SAM) techniques.

In any NEE or NEA, the spatial distribution of the individual nanoelectrodes is crucial for preventing diffusion boundary layer overlap and for the ensemble or array to behave as a nanoelectrode.<sup>5,10</sup> Here, we demonstrate a novel strategy for engineering the interelectrode spacing in the fabrication of a NEE or NEA by using the conical morphologies of carbon nanostructures termed earlier as carbon nanopipettes (CNPs). CNPs are tapered structures measuring from hundreds of nanometers (nm) up to a micrometer ( $\mu\text{m}$ ) at their bases to approximately 10 to 15 nm at their tips with lengths spanning several micrometers.<sup>11</sup> The conical geometry causes CNPs to exhibit an increased spacing at their tips compared to the close proximities of their bases. Consequently, a simple NEE fabrication technique involving the dip-coating of the ensemble with a dielectric, polymeric layer can be employed to control the spatial distribution of the exposed portions of CNPs as illustrated in Fig. 1.

This simple concept for NEE fabrication could easily be extended to other electrically conducting nanomaterials that exhibit conical morphologies similar to CNPs. Furthermore, CNP arrays could serve as templates onto which other materials could be depos-

ited or synthesized to yield conical forms of a variety of materials. These new conical arrays could then be filled with polymer or another insulator to obtain NEEs made of different materials.

CNPs possess other properties besides their tapered geometries and nanoscale tips that make them attractive as nanoelectrode materials. First, the outer edges of CNPs are composed of helical, wrapped up graphite sheets that yield a high density of exposed graphite edge planes along their tips and walls.<sup>11</sup> Graphite edge planes are favorable for electrochemistry because they yield fast electron transfer rates<sup>12</sup> and electrochemically reversible behavior for a variety of analytes including catechols and quinones.<sup>13</sup> In contrast, the sidewalls of carbon nanotubes CNTs are comprised of graphite basal planes that exhibit relatively slow electron transfer kinetics.<sup>14</sup> Additionally, CNPs do not possess metal contamination at their tips that must be removed after synthesis unlike their CNT counterparts. Furthermore, CNPs are grown on platinum (Pt) substrates, inherently providing an electrical contact for electrochemical measurements.

Therefore, CNPs are a new nanoelectrode material superior to CNTs and possess tapered morphologies. This conical geometry permits a simple polymer filling procedure to create well-spaced NEEs that behave as a single nanoelectrode. In this paper, we demonstrate the simple NEE fabrication procedure and investigate the electrochemical behavior of both the fabricated CNP NEEs and the as-synthesized, uncoated CNP array electrodes.

CNP synthesis was performed in an ASTeX model 5010 microwave (MW) plasma-enhanced chemical vapor deposition (PECVD) reactor. Pt wire substrates 0.3 mm in diameter were vertically immersed into 2%  $\text{CH}_4/\text{H}_2$  plasma using 650 W MW power at 30 Torr pressure for approximately 1 h.

Next, the as-synthesized CNPs were dip-coated with polymer to increase their spatial distribution by leaving only the isolated tips protruding from the polymer. An ultraviolet (UV) light-curable acrylate monomer solution containing photoinitiator was employed for dip-coating followed by immediate exposure to UV light flashes to cure the monomer to polymer. The monomer mixture was diluted to 50% in ethanol and was composed of the following chemicals (all weight%) available from Sartomer Company (USA): 27% CN120, 9% SR399, 27% SR454, 27% SR9003, and 10% SR1120 and benzophenone (UV photoinitiators). The insulating polymer layer served two purposes. Its first purpose was to blank out the CNP bases and the underlying carbon between them to leave only the well-spaced tips exposed. Second, the polymer passivation layer insulated the Pt substrate, except an area reserved for an electrical contact.

In order to prevent diffusion boundary layer overlap in the NEEs, the interelectrode separation must be at least twice the boundary layer thickness.<sup>9</sup> Diffusion boundary layers are established around the nanoelectrodes in a NEE as analyte molecules react at their surfaces setting up concentration profiles for diffusion to occur.<sup>4</sup> Although CNPs most closely resemble conical electrodes, their tips

\* Electrochemical Society Active Member.

<sup>c</sup> Present address: Department of Chemical Engineering, Stanford University, Stanford, CA 94305.

<sup>d</sup> Present address: Department of Chemical Engineering, University of California, Santa Barbara, Santa Barbara, CA 93106.

<sup>z</sup> E-mail: mahendra@louisville.edu

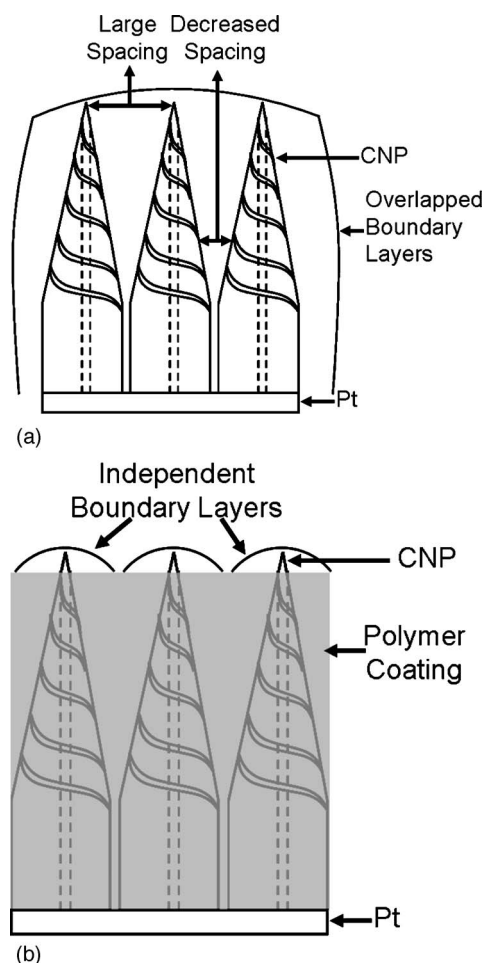


**Figure 1.** NEE fabrication concept. (a) An uncoated, as-synthesized CNP ensemble experiences diffusion boundary layer overlap because the CNPs are spaced too closely at their bases. (b) A CNP NEE after polymer coating that has left only the well-spaced tips exposed, which allows independent boundary layers to develop at each CNP.

were approximated as spherical electrodes for simplicity in estimating boundary layer thicknesses. This is a reasonable simplification at least for the purpose of estimating boundary layer thicknesses according to Zoski et al.<sup>15</sup> Fick's second law in spherical coordinates is

$$C(r,t) = C_b \left[ 1 - \frac{r_0}{r} \operatorname{erfc} \left( \frac{r - r_0}{2\sqrt{Dt}} \right) \right] \quad [1]$$

where  $C$  is the concentration at any  $r$  and  $t$ ,  $C_b$  is the bulk concentration of the analyte in solution,  $r_0$  is the electrode radius,  $r$  is the radial distance from the electrode center,  $D$  is the diffusion coefficient, and  $t$  is the time.<sup>16</sup> For CNPs, the boundary layers at  $C$  equal to 99%  $C_b$  are approximately 1 to 2  $\mu\text{m}$  thick using the following parameters:  $t = 0.1$  s,  $D = 10^{-9}$   $\text{m}^2/\text{s}$ , and  $r_0 \approx 10$  to 20 nm. Therefore, 2 to 4  $\mu\text{m}$  of spacing between individual CNPs are required for independent diffusion regimes to be established at each CNP in the NEEs. When the boundary layers overlap semi-infinite, planar diffusion occurs and leads to macro or planar electrode behavior in CV.<sup>1</sup> Whenever the boundary layers are independent and do not overlap, radial diffusion dominates and the NEE behaves as a single nanoelectrode.<sup>9</sup>

Scanning electron microscopy (SEM) was employed to monitor the increase in CNP spacing as polymer coatings were applied. Figure 2a is an SEM image of an as-synthesized, uncoated CNP array on a Pt wire. As seen in the image, the CNPs taper from large bases

where they are very dense and indistinguishable to sharp, well-spaced tips. The CNPs are oriented radially outwards from their Pt wire substrates, which is advantageous to our fabrication approach. Figure 2b represents a partially embedded CNP sample after a few micrometers of polymer have been applied. Clearly, the CNP density has decreased compared to an uncoated sample, but the spacing is still not sufficient. Although some CNPs in Fig. 2b are separated by a few micrometers, there are enough CNPs with active areas spaced closely to prevent the electrode from exhibiting nanoelectrode behavior. Figure 2c is a higher magnification SEM image of a partially embedded sample showing two adjacent CNPs protruding from the underlying polymer layer. The quality of the polymer thin film in terms of sealing around the individual CNPs and lack of defects such as holes and cracks is evident in this image. Figure 2d shows a CNP NEE after additional polymer application, which has left only the CNP tips protruding from the polymer. The spacings between CNP tips in this image are quite large enough (several micrometers) rendering independent diffusion regimes to the CNPs and nanoelectrode behavior to the overall NEE.

Cyclic voltammetry (CV) was utilized to test the electrochemical responses of the NEEs in model electrochemical analytes such as dopamine and potassium ferricyanide,  $\text{K}_3\text{Fe}(\text{CN})_6$ . Three electrodes were employed during the CV experiments, a working electrode (CNP NEE), an auxiliary electrode (Pt wire), and a reference electrode (Ag/AgCl). All measurements were performed on a Bioanalytical Systems CV-50W potentiostat.

We have demonstrated the ability to tune the electrochemical behavior of as-synthesized CNPs from planar electrodes to nanoelectrodes with the application of an insulating polymer as shown in Fig. 3, which presents voltammograms for uncoated and coated CNP electrodes. Figures 3a, b, and c correspond to the SEM images in Fig. 2a, b, and c, and d, respectively.

Figure 3a is a CV of an as-synthesized, uncoated CNP ensemble. A pair of peaks is visible at about 200 mV potential indicating the redox reactions of  $\text{K}_3\text{Fe}(\text{CN})_6$ . Positive and negative currents correspond to reduction and oxidation reactions, respectively. The peak-shaped behavior of the CV in Fig. 3a is characteristic of a solid macroelectrode and is explained by the semi-infinite, planar diffusion occurring at the electrode that results from overlapping boundary layers.<sup>5</sup> Figure 3b is a CV for a polymer-coated CNP electrode. The currents in the voltammogram are two orders of magnitude lower than for the uncoated electrode because the electrode area has been decreased from polymer coating. The reduction peak seen in Fig. 3a is no longer present in Fig. 3b, but there is still an oxidation peak present. The disappearance of the reduction peak and the resemblance of the voltammogram to a more sigmoidal shape compared to the uncoated electrode indicate the onset of nanoelectrode behavior. However, the presence of the oxidation peak means that the interelectrode tip spacing needs to be larger. Martin and coworkers observed similar responses intermediately between planar and nanoelectrode behavior with NEEs fabricated from membrane templates.<sup>17</sup>

After more polymer was applied leaving only the isolated CNP tips exposed, a steady-state voltammogram was obtained as seen in Fig. 3c. According to Zoski et al, a conical nanoelectrode should also yield a steady-state voltammogram as seen in Fig. 3c.<sup>15</sup> The sigmoidal shape in the figure provides confirmation that the CNPs are performing as individual nanoelectrodes in the ensemble.<sup>5</sup> The interelectrode spacing in the NEE in Fig. 3c allows for independent, radial diffusion regimes to be established at the CNPs in the ensemble giving rise to the steady-state, diffusion-limited plateau observed.<sup>1</sup>

Ideally, the forward (negative direction) and reverse (positive direction) scans should be superimposable. However, the NEE in Fig. 3c exhibits displacement between forward and reverse scanning and indicates that there is some degree of concentration boundary layer interaction between the CNPs in the NEE, which results from inhomogeneity in the electrode distribution.<sup>18</sup> The term NEEs is employed here rather than nanoelectrode arrays (NEAs) because the

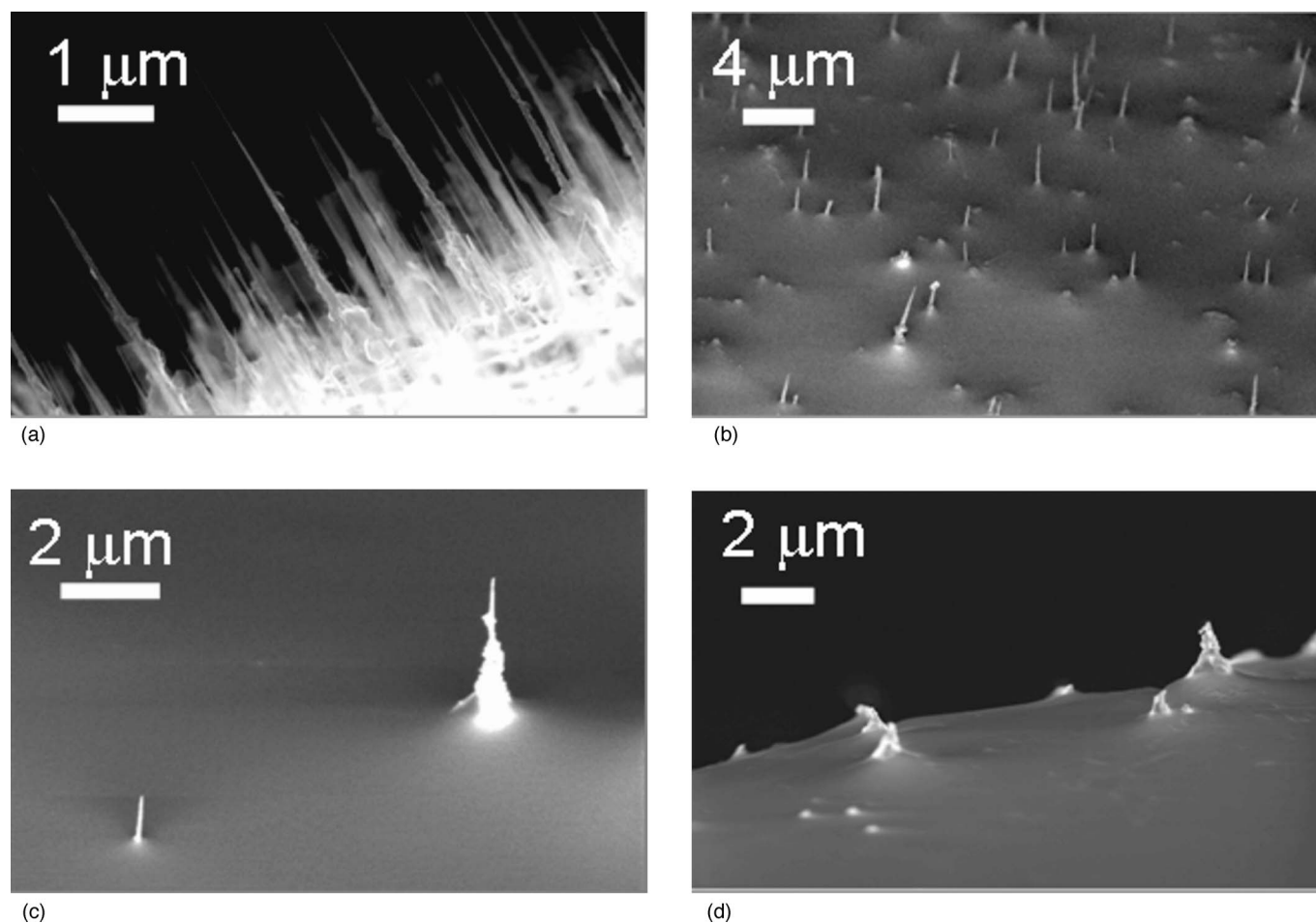


**Figure 2.** SEM images of CNP ensembles: as-synthesized with no polymer coating (a), partially embedded in polymer (b) and (c), and nearly encapsulated with additional polymer coating leaving only the tips of the CNPs exposed (d). Figures (a) through (c) behaved as planar electrodes in CV because many of the CNPs are spaced too closely. The NEE in (d) is sufficiently coated with polymer to achieve the few micrometers of spacing needed between adjacent CNPs to prevent boundary layer overlap.

individual electrodes in NEAs possess a regular, ordered spatial distribution; whereas, the nanoelectrodes in NEEs are randomly spaced as in the case of the CNP samples synthesized for this study.<sup>1,9</sup>

The performance of the fabricated CNP NEEs at varying scan rates further substantiates the claim that nanoelectrode behavior was achieved. Figure 4a shows results from varying the scan rate in CV for an uncoated CNP array, and Fig. 4b represents a polymer-coated, low-density CNP NEE for scan rates ranging from 10 to 400 mV/s. In Fig. 4a, the uncoated array exhibits planar electrode behavior with peak-shaped responses and increasing peak currents at higher scan rates. Figure 4c is a plot of the log of peak or plateau current,  $i_D$ , vs the log of the scan rate,  $v$ , over four orders of magnitude from 10 mV/s to 10 V/s. The data for the uncoated CNP array having overlapping diffusion boundary layers are linear with a slope of 0.48, very close to the expected value of 0.5 predicted from the Cottrell equation.<sup>19</sup>

On the other hand, the polymer-coated CNP NEE represented in Fig. 4b yields a sigmoidal response with a diffusion-limited, steady-state current that just slightly increases with scan rate. The sigmoidal shape was preserved even though the scan rate was varied over four orders of magnitude. The data in Fig. 4c for the coated CNP NEE are linear just as they are for the uncoated array, but the slope is 0.07 compared to 0.48 for the planar electrode. For a nanoelectrode exhibiting a steady-state current, the slope should be zero.<sup>19</sup> Therefore, there is some nonideality in the behavior of the NEEs that could result from partial boundary layer overlap or solution leakage

through the polymer passivation layer.<sup>3</sup> However, Koehne et al. reported a greater slope of 0.13 over the same range of scan rates using microfabricated CNT NEAs.<sup>5</sup>

Four CNP NEEs were made for this study, demonstrating that the fabrication concept is qualitatively reproducible. In addition, the CNP NEEs exhibited short and long-term stabilities during tests in which they were scanned 100 times continuously and over a 35-day period during which 800 CV scans were performed, respectively. Voltammograms exhibiting the reproducibility and stability of CNP NEEs are provided in the supplementary information.

Nanoelectrodes have direct applications as in vivo sensors for the detection of biologically significant analytes such as the neurotransmitter dopamine.<sup>8</sup> Ascorbic acid presents a challenge for the use of CNPs as an in vivo dopamine electrochemical sensor since it oxidizes at nearly the same potential as dopamine, resulting in only one oxidation peak at approximately 200 mV. However, we were able to resolve individual dopamine and ascorbic acid peaks with an uncoated CNP array by employing a one-time anodic oxidation treatment of the electrode at 2.0 V potential vs Ag/AgCl in 0.5 M H<sub>2</sub>SO<sub>4</sub> to shift the ascorbic acid peak while leaving the dopamine peak intact. This was the same treatment used by Mani et al. for a nanocrystalline graphite electrode.<sup>13</sup> See Fig. 5 for a CV demonstrating this treatment in obtaining separate ascorbic acid and dopamine peaks. CVs of the electrode prior to treatment are included in the

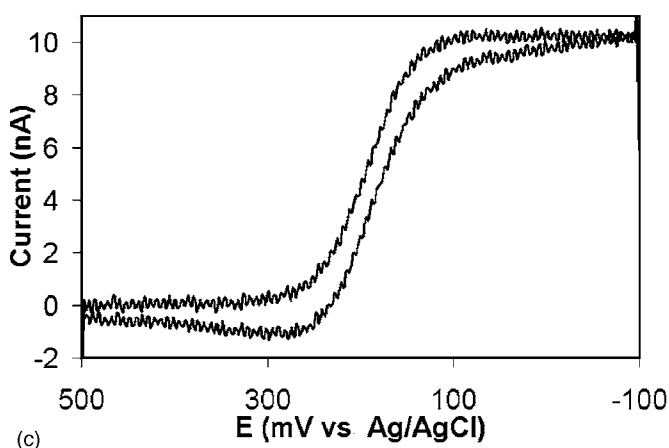
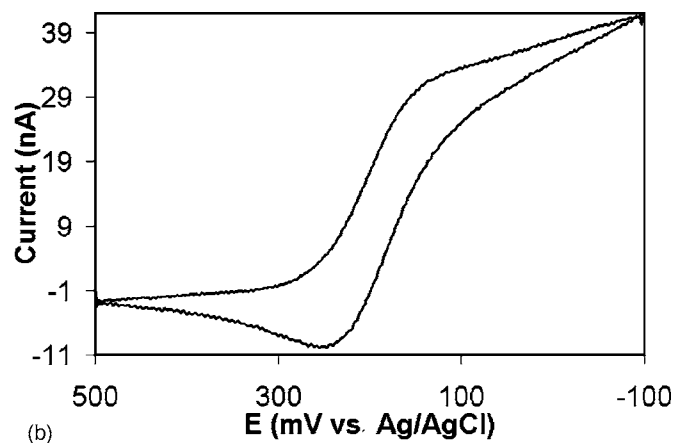
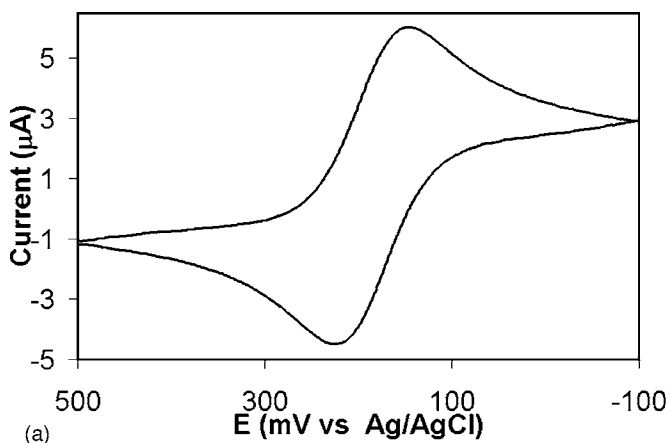


**Figure 3.** CV of CNP electrodes in 1 mM  $K_3Fe(CN)_6$  and 0.1 M KCl at 400 mV/s scan rates with: (a, top left) no polymer coating, (b, above) some polymer coating, and (c, left) additional polymer coating. The peak-shaped response in (a) is characteristic of planar electrode behavior. As polymer is applied the spatial distribution of the ensemble increases, and the electrode performance transitions to nanoelectrode behavior. This is demonstrated as the peaks begin to disappear as in (b) until finally a steady-state voltammogram is obtained as in (c) when diffusion boundary layer overlap is minimized.

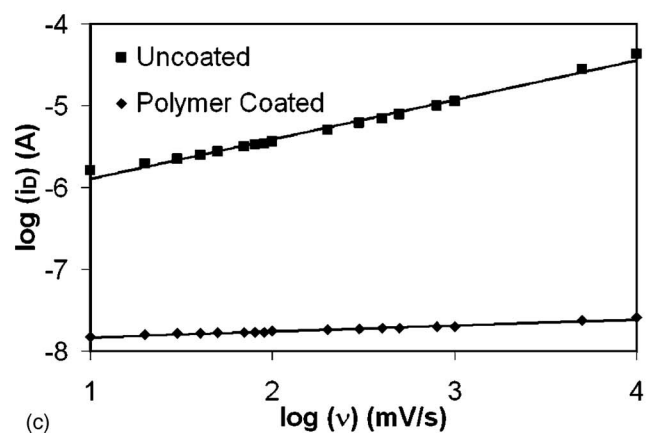
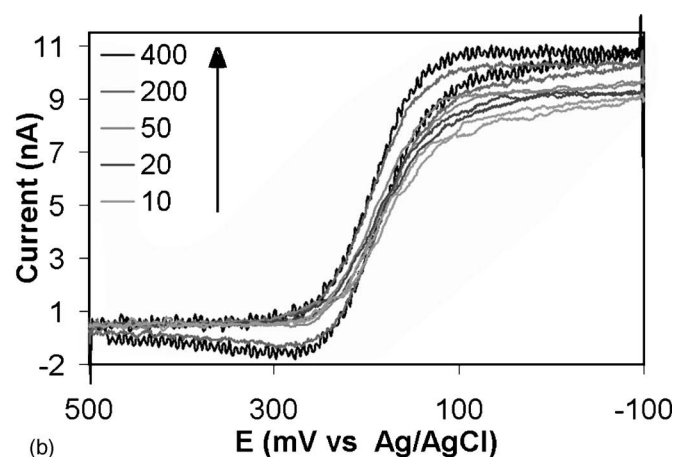
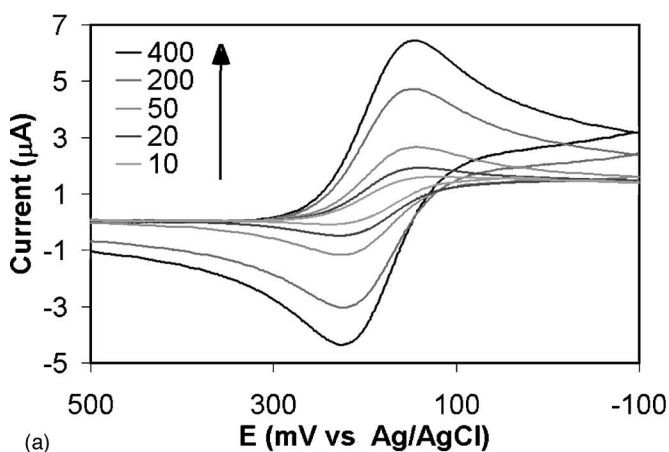


**Figure 4.** CV at 10 to 400 mV/s scan rates for an uncoated CNP array (a, top left) exhibiting planar electrode behavior with peak-shaped responses and for a polymer-coated CNP NEE, (b, above) yielding sigmoidal curves with steady-state, diffusion-limited currents, (c, left) is a plot of the log of peak or plateau current vs the log of scan rate over four orders of magnitude from 10 mV/s to 10 V/s for an uncoated CNP array (top) and a polymer-coated NEA (bottom). The data fit a linear trend with slopes of 0.48 and 0.07 for the uncoated and coated CNP arrays, respectively.

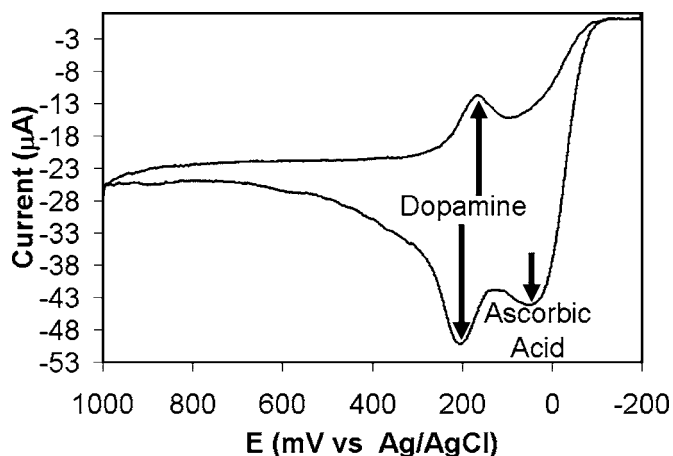


**Figure 5.** CV of an uncoated CNP electrode at 100 mV/s scan rate in a 0.1 mM dopamine and 10 mM ascorbic acid solution in 0.1 M KCl in 0.2 M phosphate buffer solution, pH 7, after a single anodic oxidation treatment. This same treatment could be extended to CNP NEEs and render two oxidation plateau currents for dopamine/ascorbic acid mixtures.

supplementary information. The CNP NEEs could also be treated to yield two plateaus for a mixture of ascorbic acid and dopamine, but we have not yet achieved this result.

In summary, we have developed a simple technique for controlling the individual spacing of structures exhibiting conical, tapered geometries such as CNPs in the fabrication of a NEE or NEA that avoids the complexities of methods involving microfabrication, template-assisted, or SAMs. Adequate spacing in a NEA or NEE is crucial to ensure that each element behaves as a single nanoelectrode. As expected for conical electrodes, the CNP NEEs exhibited steady-state, diffusion-limited currents during CV. CNP NEEs exhibited both short-term and long-term stabilities. It was demonstrated that one can reliably manipulate the electrochemical perfor-

mance of CNP electrodes from planar to nanoelectrode behavior with the quick application of an insulating polymer coating. This NEE fabrication concept can be applied to a variety of structures similar to CNPs that exhibit tapered morphologies, which automatically results in well-separated tips important for applications such as nanoarray electrochemical sensing and field emission.

#### Acknowledgments

Financial support from a Kentucky Space Grant Consortium (KSGC) fellowship is gratefully acknowledged.

University of Louisville assisted in meeting the publication costs of this article.

#### References

1. D. W. M. Arrigan, *Analyst (Cambridge, U.K.)*, **129**, 1157 (2004).
2. D. K. Y. Wong and L. Y. F. Xu, *Anal. Chem.*, **67**, 4086 (1995).
3. Y. Tu, Y. Lin, and Z. F. Ren, *Nano Lett.*, **3**, 107 (2003).
4. K. Stulik, C. Amatore, K. Holub, V. Marecek, and W. Kutner, *Pure Appl. Chem.*, **72**, 1483 (2000).
5. J. Koehne, J. Li, A. M. Cassell, H. Chen, Q. Te, H. T. Ng, J. Han, and M. Meyyappan, *J. Mater. Chem.*, **14**, 676 (2004).
6. J. Heinze, *Angew. Chem., Int. Ed. Engl.*, **32**, 1268 (1993).
7. R. M. Penner, M. J. Heben, T. L. Longin, and N. S. Lewis, *Science*, **250**, 1118 (1990).
8. B. J. Venton and R. M. Wightman, *Anal. Chem.*, **75**, 414A (2003).
9. P. Ugo, L. M. Moretto, and F. Vezza, *ChemPhysChem*, **3**, 917 (2002).
10. Y. Lin, F. Lu, Y. Tu, and Z. Ren, *Nano Lett.*, **4**, 191 (2004).
11. R. C. Mani, X. Li, M. K. Sunkara, and K. Rajan, *Nano Lett.*, **3**, 671 (2003).
12. J. M. Nugent, K. S. V. Santhanam, A. Rubio, and P. M. Ajayan, *Nano Lett.*, **1**, 87 (2001).
13. R. C. Mani, M. K. Sunkara, R. P. Baldwin, J. Gullapalli, J. A. Chaney, G. Bhimarasetti, J. M. Cowley, A. M. Rao, and R. Rao, *J. Electrochem. Soc.*, **152**, E154 (2005).
14. J. Li, H. T. Ng, A. Cassell, W. Fan, H. Chen, Q. Ye, J. Koehne, J. Han, and M. Meyyappan, *Nano Lett.*, **3**, 597 (2003).
15. C. G. Zoski and M. V. Mirkin, *Anal. Chem.*, **74**, 1986 (2002).
16. A. J. Bard and L. R. Faulker, *Electrochemical Methods: Fundamentals and Applications*, 2nd ed., p. 165, Wiley, New York (2001).
17. J. C. Hulteen, V. P. Menon, and C. R. Martin, *J. Chem. Soc., Faraday Trans.*, **92**, 4029 (1996).
18. W. S. Baker and R. M. Crooks, *J. Phys. Chem. B*, **102**, 10041 (1998).
19. P. H. Rieger, *Electrochemistry*, 2nd ed., p. 151, Chapman & Hal, New York (1994).